FORWARD JET AND PARTICLE PRODUCTION AT LOW X

L. JÖNSSON*

Physics Department, Lund University
Box 118,
S-221 00 Lund, Sweden
E-mail: leif.jonsson@hep.lu.se

In the kinematic region where the partons carry a very small fraction of the proton momentum their dynamics is expected to be characterized by initial state cascades which are non-ordered in virtuality of the propagators. In electron-proton collisions the investigation of jet- and single particle production along the direction of the incoming proton provides high sensitivity to such effects. Some recent experimental results from HERA are presented and compared to next-to-leading order calculations and to different QCD models in order to find evidence for the new effects.

1. Introduction

Quantum Chromodynamics (QCD) is generally regarded to be the correct theory to describe interactions between the quarks, which to our present knowledge are the smallest building blocks of matter. So far QCD has been mainly applicable to explain experimental data from hard scattering processes, where the relevant degrees of freedom are the fundamental particles, quarks and gluons. Although QCD has been successful in describing much data from deep inelastic scattering (DIS) we still face a number of problems like the description of parton dynamics at very small x-values, saturation effects, shadowing phenomena etc. A better understanding of the transition region between short- and long-range physics as well as of the long-range physics itself, and a theoretical description of such processes within the framework of QCD, is one of the most interesting challenges for the future.

Collisions between electrons and protons offer unique possibilities to study the partonic structure of matter. A particular advantage is that in

*Representing the H1 and ZEUS collaborations such collisions the hardness of the interaction can be varied by selecting the energy and virtuality of the exchanged photon. With the higher resolution achieved by larger photon virtuality or with larger photon energy, a quark or a gluon can be resolved into a cascade of gradually softer partons. Various approximation schemes have been developed to calculate the evolution of parton cascades. For large photon virtualities the DGLAP evolution scheme [1] is applicable, whereas for very large photon energies the BFKL scheme [2] is relevant. The HERA facility offers the presently highest energies for performing such studies.

One of the most striking observations from the HERA experiments is the sharply rising density of quarks and gluons as the resolving power of the exchanged photon is increased, giving sensitivity to quarks carrying a very small fraction of the parton momentum. This strong rise was rather unexpected, although it was actually predicted by the BFKL formalism. It is clear that this rise of the parton density can not continue beyond limits, since it would ultimately lead to a violation of the unitarity principle, which guarantees that the total reaction probability must be smaller than 1. Thus, for sufficiently small x-values the density of partons becomes so large that they start to recombine. This saturation effect may be within reach at HERA, but it is also possible that the higher energies expected at future colliders are needed.

The dependence of the parton distribution on the energy fraction, x, carried by the parton and of the photon virtuality, Q^2, is one of the most interesting and challenging problems in QCD. This problem is intimately related to such diverse phenomena as shadowing in deep inelastic lepton-nucleon scattering, the amount of energy produced in the central region of heavy ion collisions and perhaps even to the growth of the total hadronic cross section at ultra high energies.

2. QCD models

The basic, or lowest order, parton level process must be corrected for higher order perturbative QCD effects causing the emission of extra partons on a short space-time scale. These can either be calculated by exact matrix elements, which has so far only been possible to low orders in the strong coupling constant, α_s, or approximately by parton cascades based on the iteration (to arbitrary orders in α_s) of the basic quark (q) and gluon (g) radiation processes $q \to qg$, $g \to gg$ and $g \to q\bar{q}$. Fixed order QCD calculations are available up to next-to-leading order (NLO) in the case of inclusive jet production at HERA. It is, however, important to keep in mind that the question to which order in α_s a calculation has been performed depends on the observable. For example leading order (LO) is different in a measurement of inclusive jet production compared to di-jet production. LO is thus the lowest order in which the observable obtains a non-zero value, and NLO is the next higher order. For DIS processes there are four programs existing, which provide matrix element calculations up to NLO. These are DISENT [3] , DISASTER++ [4] , MEPJET [5] and JetViP [6] .

At high energies the interactions leave a large phase space for parton emission. Higher order QCD effects will therefore become important and to account for these it is necessary to use phenomenological parton shower models. There are various models on the market with different formulations of the basic evolution equations for parton branchings, and therefore the models are valid in certain regions of phase space only.

2.1. *The DGLAP model*

The DGLAP evolution equation is of the form

$$\frac{df_j(x,\mu^2)}{d\ln\mu^2} = \frac{\alpha_s(\mu^2)}{2\pi}\sum_i \int_x^1 \frac{dx'}{x'} f_i(x',\mu^2) P_{i\to j,k}(z) \tag{1}$$

where $f(x,\mu^2)$ is the density of partons carrying a longitudinal momentum fraction x probed at a scale μ^2, and $P_{i\to j,k}(z)$ describes the probability that a parton i is split into two partons j and k with a fraction $z = \frac{x}{x'}$ and $1-z$ of the original parton momentum, respectively. The probability that a gluon splits into two gluons is given by

$$P_{g\to g,g}(z) = \frac{1}{1-z} - 2 + z(1-z) + \frac{1}{z} \tag{2}$$

where the terms $\frac{1}{1-z}$ and $\frac{1}{z}$ are called singular terms, since they give infinite contributions when $z \to 1$ and $z \to 0$, respectively. Equation (1) thus describes the probability change of finding a parton of type j with momentum fraction x as we increase the scale μ^2. In the DGLAP formalism, the propagator gluons are assumed to be strongly ordered in virtuality

$$\mu^2 \gg |k_n^2| \ldots \gg |k_i^2| \ldots \gg |k_1^2| \gg |k_0^2|, \tag{3}$$

where k_i is the four momentum of parton i. It can be shown that the ordering in virtuality implies that also the transverse momentum of the propagator partons (at small x) has to be strongly ordered according to

$$\mu^2 \gg |k_{tn}^2| \ldots \gg |k_{ti}^2| \ldots \gg |k_{t1}^2| \gg |k_{t0}^2| \tag{4}$$

Since the virtualities and transverse momenta of all the gluon propagators are small compared to the hard scale, μ^2, they can be treated as massless and approximated to move in the same direction as the incoming proton (collinear approximation). It can be shown, that the DGLAP evolution gives a resummation of terms of the form $(\alpha_s \ln(\mu^2))^n$ in the expansion of the cross section. Hence, the DGLAP approximation is only valid at large μ^2 where these terms will dominate.

In electron-proton scattering the internal structure of the proton as well as of the exchanged photon can be resolved provided the scale of the hard process is larger than the inverse radius of the proton, $1/R_p^2 \sim \Lambda_{QCD}^2$, and the photon, $1/R_\gamma^2 \sim Q^2$, respectively. Resolved photon processes play an important role in photo-production of high p_t-jets, since $Q^2 = 0$, but they can also give considerable contributions to DIS processes if the scale μ^2 of the hard subprocess is larger than Q^2. This situation can be described by introducing two DGLAP ladders, one from the proton side and another from the photon side [7].

2.2. *The BFKL model*

The BFKL evolution equation resums the terms $(\alpha_s \ln(\frac{1}{x}))^n$ in the expansion, and is thus only valid at small x. Thus, the evolution is made in increasing $\ln(\frac{1}{x})$, since

$$x_0^2 \gg x_1^2 \ldots \gg x_n^2 \gg x_{Bj}^2 \tag{5}$$

has been assumed. This implies that the emitted gluons will take a large fraction of the propagator momentum. However, there is no restriction in k^2 or k_t^2. This means that the virtualities and transverse momenta of the propagators can take any kinematically allowed value and must not be smaller than the photon virtuality as was the case in the DGLAP description. Consequently the collinear approach is no longer applicable but the matrix elements must be taken off mass shell (the particles can have virtual mass) and unintegrated parton densities, taking the transverse momenta of the propagators into account, have to be used. This is called k_t-factorisation [8]. The BFKL evolution equation is of the form

$$\frac{d\mathcal{G}(x, k_t^2)}{d\ln(\frac{1}{x})} = \int dk_t^{'2} \mathcal{G}(x, k_t^{'2}) \cdot K(k_t^2, k_t^{'2}) \tag{6}$$

where

$$\mathcal{G}(x, k_t^2) \cong \left. \frac{dg(x, \mu^2)}{d\mu^2} \right|_{\mu^2 = k_t^2} \tag{7}$$

with

$$g(x, \mu^2) \simeq \int_0^{\mu^2} dk_t^2 \mathcal{A}(x, k_t^2, \mu^2). \qquad (8)$$

$\mathcal{A}(x, k_t^2, \mu^2)$ is the unintegrated gluon density describing the probability to find a gluon with a longitudinal momentum fraction x and a transverse momentum k_t at a scale μ^2. The function K is the splitting kernel equivalent to P in (1). To distinguish the different parton distributions, the following notation has been used: $g(x, \mu^2)$ is the parton distribution in the collinear approach, while $\mathcal{G}(x, k_t^2)$ and $\mathcal{A}(x, k_t^2, \mu^2)$ are the one- and two-scale distributions in the k_t-factorization approach.

2.3. *The CCFM model*

The CCFM [9] evolution equation is valid both at large and small x, since it resums terms of both the form $(\alpha_s \ln(\frac{1}{x}))^n$ and $(\alpha_s \ln(\frac{1}{1-x}))^n$. This means that at large x the CCFM evolution will be DGLAP-like, and at small x it will be BFKL-like. The CCFM evolution includes angular ordering in the initial state cascade, to account for colour coherence effects, which means that the emission angles of the partons with respect to the incoming proton increases as one moves towards the quark box,

$$\Xi \gg \xi_n \gg \ldots \ \xi_1 \gg \xi_0, \qquad (9)$$

where the maximum allowed angle Ξ is set by the hard quark box.

The original CCFM splitting function $\tilde{P}$ was defined as

$$\tilde{P}_g(z, k_t^2, \bar{q}) = \frac{\bar{\alpha}_s(\bar{q}_i^2)}{1 - z_i} + \frac{\bar{\alpha}_s(k_{ti}^2)}{z_i} \Delta_{ns}(z_i, k_{ti}^2, \bar{q}_i^2), \qquad (10)$$

where

$$\bar{q}_i = \frac{p_{ti}}{1 - z_i} = x_{i-1}\sqrt{s\xi_i}$$

is the rescaled transverse momenta of the emitted gluons and $z_i = \frac{x_i}{x_{i-1}}$. The CCFM splitting function differs from the DGLAP splitting function in the sense that it only includes the singular terms. Another difference is the additional function Δ_{ns}, called the non-Sudakov form factor. The non-Sudakov form factor originates from the fact that, in CCFM and BFKL, all virtual corrections in the gluon vertex are automatically taken into account. This is called the Reggeization of the gluon vertex.

At very high energies the $1/z$-term in the splitting function will dominate and it is sufficient to include the singular terms. However, for the energies at present colliders it is still necessary to take the non-singular terms into account in the splitting function, which then takes the form:

$$\tilde{P}_g(z, k_t^2, \bar{q}) = \bar{\alpha}_s(\bar{q}_i^2)\left(\frac{z_i}{1-z_i} + \frac{z_i(1-z_i)}{2}\right) + \bar{\alpha}_s(k_{ti}^2)\left(\frac{(1-z_i)}{z_i} + \frac{z_i(1-z_i)}{2}\right)\Delta_{ns} \tag{11}$$

2.4. *The Colour Dipole Model*

In the Colour Dipole Model (CDM) [10] the emissions are assumed to originate from colour dipoles streched between the partons. The primordial dipole is spanned between the scattered quark and the proton remnant. The emission of a gluon by this dipole produces a 'kink' in the dipole leading to secondary dipoles, which may in turn produce further dipoles by emitting more gluons. Since the dipoles are radiating independently, the parton cascade will not be ordered in transverse momentum and therefore exhibit a BFKL-like behaviour. The fact that the proton remnant is an extended object will reduce the phase space for gluon emission because the gluon can only access a fraction of the momentum carried by the proton remnant. In a resolved photon case the photon can also be regarded as an extended object, described by its parton density functions just like the proton, and thus a similar suppression is obtained on the photon side.

3. Inclusive jet production

In the region of low x-values the interacting parton frequently produces a cascade of emissions before it interacts with the virtual photon. Due to the strong ordering in virtuality, the emissions of the DGLAP evolution are very soft close to the proton direction, whereas BFKL emissions can produce large transverse momenta in this region. Thus, deviations from the DGLAP parton evolution scheme are expected to be most visible in a region close to the direction of the incoming proton. The ZEUS collaboration has studied inclusive jet production in DIS at photon virtualities, $Q^2 > 25\ GeV^2$, and x-values down to $7 \cdot 10^{-4}$ in order to investigate whether deviations from the DGLAP picture could be observed, which could then be better described by the BFKL model.

The jet search was performed by applying the longitudinally invariant k_t-algorithm to the information from the calorimeter cells. Jets were accepted provided they had a transverse energy $E_{t,jet} > 6\ GeV$ and were reconstructed inside the rapidity range $-1 < \eta_{jet} < 3$ in the laboratory system.

The data sample obtained provided the basis for two independent analyses. The first one used the full phase space as defined by the cuts given above. In the second analysis the so called hadronic angle, γ_h, was calculated from a calorimetric measurement of the hadronic final state. Only events where the momentum vector of the hadronic system was pointing in the backward direction ($\cos\gamma_h < 0$) and the jet (jets) was reconstructed in the forward part of the detector ($\eta_{jet} > 0$) were accepted in this analysis. The data sample of the first analysis was dominated by single jet events, whereas the hadronic angle restriction removed such events and enhanced the contribution from di-jet and multi-jet events in the second sample. To distiguish the two samples the first one is referred to as the 'inclusive phase space' and the second as the 'di-jet phase space'.

The differential cross section for the two samples was measured as a function of the transverse jet energy, the jet pseudorapidity, the photon virtuality and Bjorken-x. The results were compared to the predictions from NLO calculations in the DGLAP approach as given by the DISENT program and from the phenomenological descriptions given by the DGLAP evolution as implemented in the LEPTO generator [11] and by CDM in the ARIADNE program [12]. Radiative corrections were accounted for by using the DJANGO program [13], which provides an interface between the QED generator HERACLES [14] and LEPTO or ARIADNE. Hadronisation was performed using the Lund string model [15].

The results from the 'inclusive phase space' (Fig. 1) show that the description of data as η_{jet} increases becomes worse. This can be understood from the fact that the α_s^o contribution goes to zero at fixed Q^2 and x (alternatively y), since the value of η_{jet} is fixed in an α_s calculation by $\frac{1}{2}\ln\frac{Q^2(1-y)}{4E_e^2y^2}$. Experimentally a certain range in Q^2 is covered which obviously influences the maximum value of η_{jet}. In the kinematic region chosen by ZEUS the maximum η_{jet} is around 1 and this is also where NLO calculations start deviating from data. Both CDM (ARIADNE) and the DGLAP model (LEPTO) are in good agreement with data. The QCD models as well as NLO calculations are able to reproduce the Bjorken-x distribution down to values of about $2 \cdot 10^{-3}$ but at lower values the DGLAP model and even more the NLO calculations strongly disagree with data. All this indicates that calculations in NLO are not enough and that higher order corrections are necessary.

The jet cross section in the 'di-jet phase space' seems to be better de-

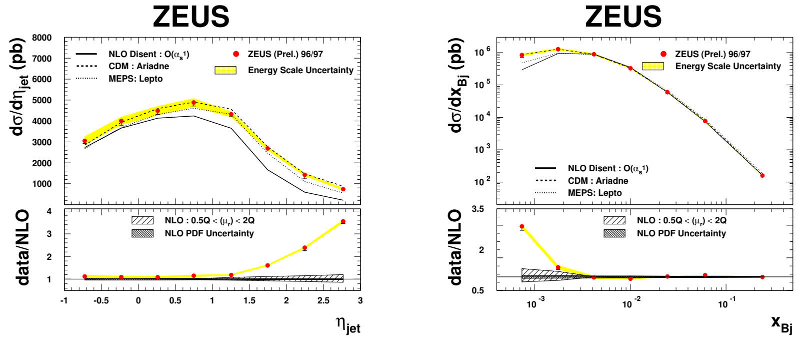

Figure 1. $d\sigma/d\eta_{jet}$ and $d\sigma/dx$ for the 'inclusive phase space' data.

scribed by NLO calculations and by the QCD models both when it is plotted as a function of η_{jet} and as a function of Bjorken-x (Fig. 2). On the other hand we can observe that the scale uncertainty has blown up which excludes any clear conclusions.

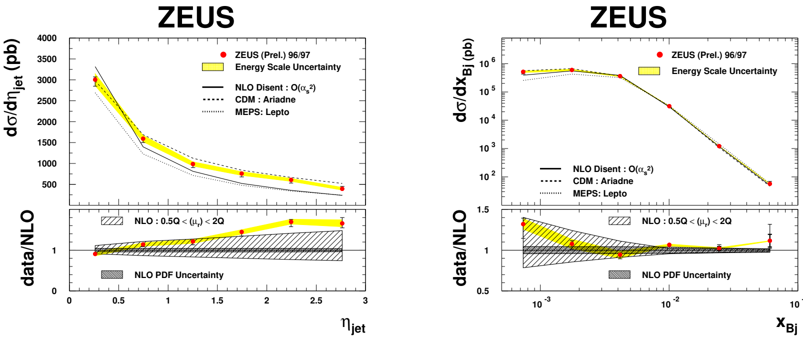

Figure 2. $d\sigma/d\eta_{jet}$ and $d\sigma/dx$ for the 'di-jet phase space' data.

It should be recalled that NLO for inclusive jet production is order α_s^1, whereas NLO for di-jet production is order α_s^2.

4. Forward jet production

A measurement of the forward jet production cross section at small Bjorken-x, as proposed by Mueller and Navelet [16], has since long been regarded as the most promising test of perturbative parton dynamics. The idea is to select events with a jet close to the proton direction having the virtuality of the propagator closest to the proton approximately equal to the virtuality of the exchanged photon. This will prevent an evolution with strong ordering in virtuality as is the case in the DGLAP evolution. The additional requirement that the forward jet takes a large fraction of the proton momentum, $x_{jet} = E_{jet}/E_p$, such that $x_{jet} \gg x_{Bj}$ opens up for an evolution where the propagators are strongly ordered in the longitudinal momentum fraction like in the BFKL scheme. Experimentally this is realized by demanding the transverse momentum of the forward jet to be of the same order as Q^2 and x_{jet} to be larger than a preselected value which still gives reasonable statistics.

The H1 experiment has recently measured the forward jet cross section from a sample of events obtained by applying the cuts $E_{e'} > 10\ GeV$, $156^o < \Theta_e < 175^o$, $0.1 < y < 0.7$ and $5 < Q^2 < 75\ GeV$. Jets were reconstructed using the inclusive k_t-algorithm in the Breit frame. In order to fulfill the conditions discussed above to suppress DGLAP and enhance BFKL evolution, it was required that $0.5 < p_t^2/Q^2 < 2$ and $x_{jet} > 0.035$. The jet angle had to be larger than 7^o with respect to the proton direction, which ensures that the jet is well inside the acceptance of the detector. Further the transverse energy of the jet had to be $p_{t,jet} > 3.5\ GeV$ to stay in the perturbative region.

The cross section of forward jet production is shown as a function of x in Fig. 3. Data are compared to the predictions of the DGLAP model with and without resolved virtual photons (DGLAP 'resolved' and DGLAP 'direct', respectively) as implemented in the RAPGAP Monte Carlo program [17]. Also shown are the predictions from CDM as given by ARIADNE and of the CCFM evolution, which has been parametrized in the CASCADE generator [18]. Three different unintegrated gluon densities were used in CASCADE. That of JS2001 was determined through a fit to the early $F_2(x, Q^2)$-data from HERA taken in 1994. The soft region was avoided by applying a cut $k_t^{cut} > 0.25\ GeV$ and collinear emissions were excluded by setting $Q_o > 1.4\ GeV$. In the CCFM evolution k_t can take any kinematically allowed value i.e. also values smaller than k_t^{cut}. In such a case no real emission is allowed in CASCADE and the evolution in angle continues until the k_t-condition is fulfilled. For the versions J2003-1 and -2 the unintegrated gluon densities have been determined from fits to the $F_2(x, Q^2)$-data obtained at HERA in 1994 and 1996/97. The input parameters of the model was defined such as to fit the data in the region $x > 5 \cdot 10^{-3}$ and $Q^2 > 4.5\ GeV^2$. J2003-1 has $k_t^{cut} = Q_o = 1.33\ GeV$, whereas J2003-2 has $k_t^{cut} = Q_o = 1.18\ GeV$. The difference between these two sets is that set 1 only includes singular terms in the splitting function whereas set 2 also takes the non-singular terms into account.

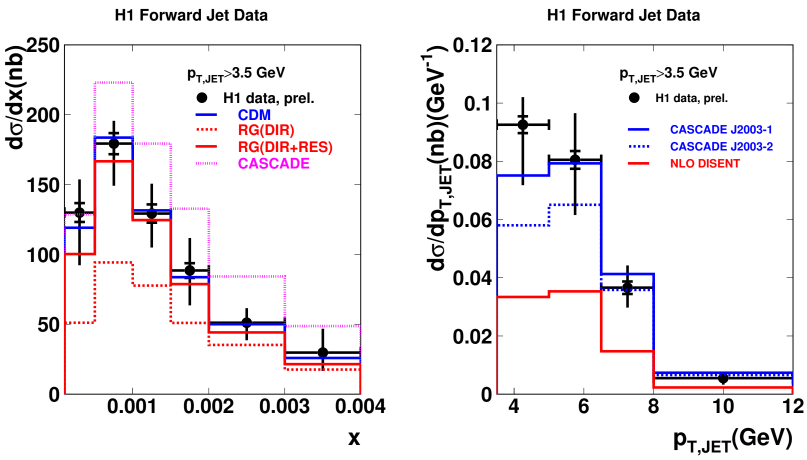

Figure 3. $d\sigma/dx$ for forward jet production compared to various QCD models (CDM, DGLAP 'direct' (RG(DIR)), DGLAP 'resolved' (RG(DIR+RES)), CCFM (CASCADE JS2001, J2003-1, J2003-2) and NLO calculations (NLO DISENT)

From Fig. 3 it is seen that DGLAP 'direct' is undershooting the data and that the contribution from resolved photons gives agreement with data. CDM describes the data well while CASCADE (JS2001) gives too high a cross section. Further the NLO calculations by DISENT give cross sections which are a factor two smaller than data. CASCADE version J2003-1 reproduces data well and J2003-2, with non-singular terms in the splitting fuction, gives a reasonable agreement although it is somewhat on the low side.

5. Forward pion production

Following the idea behind the forward jet measurement it is also possible to select high energy single particles in the forward direction and require the criteria of Mueller and Navelet to be fulfilled. The advantage of using single particles is that angles closer to the proton direction can be reached compared to jets, which have a certain lateral extension. On the other hand the cross section for events with a specific high energy forward particle is lower than the jet cross section and the sensitivity to fragmentation effects becomes higher.

The H1 collaboration has performed a measurement on single forward π^o-meson production, where the π^o-meson is identified through its dominant decay into two photons. The photons were measured in the calorimeter but due to the high energy of the pion, the photons could not be separated but were detected as one single cluster. The analysis was restricted to the kinematic range defined by the cuts $0.1 < y < 0.6$ and $2 < Q^2 < 70\ GeV^2$. The polar angle of the pion was required to be in the range $5^o < \Theta_\pi < 25^o$ with $x_\pi = E_\pi / E_p > 0.01$.

Inclusive forward π^o cross sections for $p_{t,\pi^o} > 2.5\ GeV$, measured in the proton-photon centre-of-mass system, are shown in Fig. 4 as a function of x for three different regions in Q^2. It should be noticed that the measurements extend down to $x = 4 \cdot 10^{-5}$. The results show that the prediction of DGLAP 'direct' (DIR) again is well below the data, whereas a reasonable description is obtained if the resolved photon contribution (DIR+RES) is added. Somewhat unexpectedly all sets of CASCADE (only JS2001 is shown) fall below the data at small x-values. One explanation for this could be that CASCADE produces mostly gluon jets in this region, while RAPGAP also produces quark jets. Since the fragmentation of quarks into pions has a harder spectrum the selection criteria will enhance the quark-jet contribution. It should, however, be pointed out that there is no direct contradiction since the discepancies in the π^o cross section occur in a region of x which is mostly not covered by the forward jet measurement. A comparison was also made to a modified LO BFKL calculation [19] which was supplemented by a consistency constraint to mimic higher orders in the perturbative expansion. There is good agreement between this calculation and the data.

The parton cascades from the different evolution schemes should result in transverse energy flow distributions, which are different. The π^o data have been used to study the transverse energy flow with respect to the pion in the hadronic centre-of-mass system. The results are presented for three different rapidity ranges and compared to the predictions of the QCD models in Fig. 5. The experimental distribution in the rapidity range closest to the proton direction indicates that the energy compensation occurs over

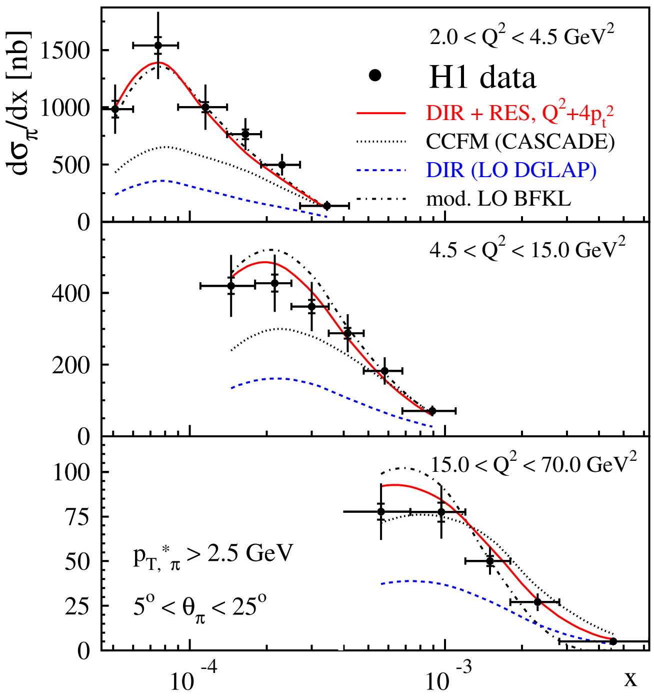

Figure 4. $d\sigma/dx$ for forward pion production compared to various QCD models (DGLAP 'direct' (DIR), DGLAP 'resolved' (DIR+RES), CCFM (CASCADE JS2001) and a modified BFKL calculation (LO BFKL).

the full length of the parton ladder, which is in disagreement with the predictions of long range compensation from DGLAP. The best description of data is given by DGLAP 'resolved'.

6. Conclusions

The production of jets and single particles in the forward region has been studied in order to search for deviations from the standard DGLAP description of the parton dynamics. Significant discrepancies between data and the simple DGLAP predictions were observed but if the exchanged photon is allowed to interact via its partonic content (resolved virtual photons) good agreement is obtained with most data. The CCFM evolution scheme, which combines the properties of DGLAP and BFKL, give similar agreement and

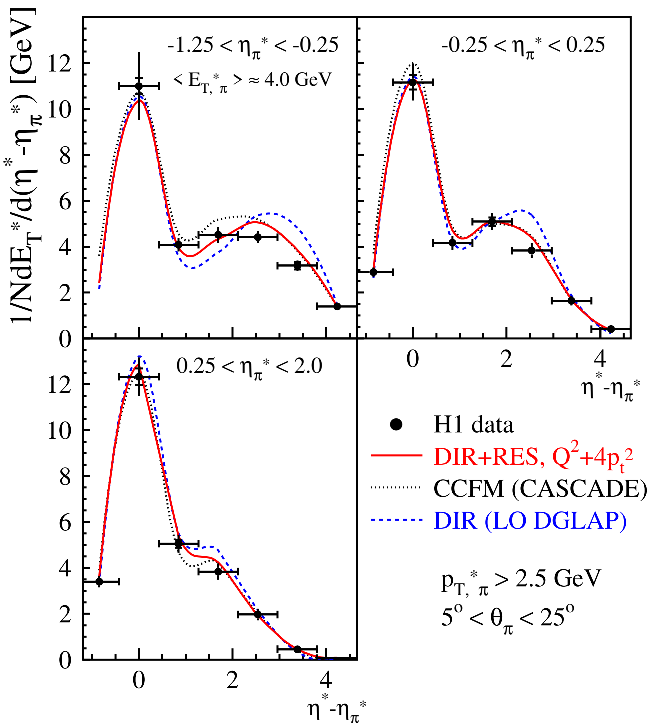

Figure 5. $1/NdE_t/d(\eta - \eta_\pi$ for forward pion production compared to various QCD models (DGLAP 'direct' (DIR), DGLAP 'resolved' (DIR+RES), CCFM (CASCADE JS2001).

has the advantage to contain less free parameters. The final conclusion is, however, that so far no clear evidence for new parton dynamics has been observed.

7. Acknowledgments

I would like to express my gratitude to the organising committee for the invitation to give this talk and for creating such a nice atmosphere during the conference. M. Klein, T. Greenshaw, P. Newman, H. Jung and J. Butterworth are acknowledged for good advises and comments in the preparation of the talk.

References

1. V. Gribov and L. Lipatov, *Sov. J. Nucl. Phys.* **15**, 438 and 675 (1972)
   L. Lipatov, *Sov. J. Nucl. Phys.* **20**, 94 (1975)
   G. Altarelli and G. Parisi, *Nucl. Phys.* **B 126**, 298 (1977)
   Y. Dokshitzer, *Sov. Phys. JETP* **46** 641 (1977)
2. E. Kuraev, L. Lipatov and V. Fadin, *Sov. Phys. JETP* **44**, 443 (1976)
   E. Kuraev, L. Lipatov and V. Fadin, *Sov. Phys. JETP* **45**, 199 (1977)
   Y. Balinsky and L. Lipatov, *Sov. J. Nucl. Phys.* **28**, 822 (1978)
3. S. Catani, M.H. Seymour, *Phys. Lett.* **B 378**, 287 (1996), *Nucl. Phys.* **B 485**, 291 (1997)
4. D. Graudenz, PSI.PR-97-20, hep-ph/979240
5. E. Mirkes, D. Zeppenfeld, *Phys. Lett.* **B 380**, 23 (1996), *Acta Phys. Polon.* **B 27**, 1392 (1996)
6. B. Pötter, *Comp. Phys. Comm.* **119**, 45 (1999)
   B. Pötter, *Comp. Phys. Comm.* **133**, 105 (2000)
7. H. Jung, L. Jönsson, H. Küster, *Eur. Phys. J.* **C 9**, 383 (1999)
8. S. Catani, M. Ciafaloni, F. Hautmann, *Nucl. Phys.* **B 366**, 135 (1991)
   J. Collins, R. Ellis, *Nucl. Phys.* **B 360**, 3 (1991)
   L. Gribov, E. Levin, M. Ryskin, *Phys. Rep.* **100**, 1 (1983)
   E.M. Levin, M.G. Ryskin, Y.M. Shabelski, A.G. Shuvaev, *Sov. J. Nucl. Phys.* **53**, 657 (1991)
9. M. Ciafaloni, *Nucl. Phys.* **B 296**, 49 (1988)
   S. Catani, F. Fiorani and G. Marchesini, *Phys. Lett.* **B 234**, 339 (1990)
   S. Catani, F. Fiorani and G. Marchesini, *Nucl. Phys.* **B 336**, 18 (1990)
   G. Marchesini, *Nucl. Phys.* **B 445**, 49 (1995)
10. G. Gustafson, *Phys. Lett.* **B 175**, 453 (1986)
    G. Gustafson, U. Pettersson *Nucl. Phys.* **C 306**, 746 (1988)
11. G. Ingelman, A. Edin and J. Rathsman, *Comp. Phys. Comm.* **101**, 108 (1997)
12. L. Lönnblad, *Comp. Phys. Comm.* **71**, 15 (1992)
    L. Lönnblad, *Z. Pys.* **C 65**, 285 (1995)
13. K. Charchula, G.A. Schuler, H. Spiesberger, *Comp. Phys. Comm.* **81**, 381 (1994)
14. A. Kwiatkowski, H. Spiesberger, H.-J. Möhring *Comp. Phys. Comm.* **69**, 155 (1992)
15. T. Sjöstrand*Comp. Phys. Comm.* **82**, 74 (1994)
16. A.Mueller, *Nucl. Phys. B* (*Proc. Suppl.*) **18C**, 125 (1990)
    A. Mueller, *J. Phys.* **G 17**, 1443 (1991)
    A. Mueller, H. Navelet, *Nucl. Phys.* **B 282**, 727 (1987)
17. H. Jung, http://www.quark.lu.se/ hannes/rapgap/
18. H. Jung, *Eur. Phys. J.* **C 19**, 351 (2001)
    H. Jung, *Comp. Phys. Comm.* **143**, 100 (2002)
19. J. Kwiecinski, A. Martin, J. Outhwait, *Eur. Phys. J.* **C 9**, 611 (1999)